



Modulation of local wind-waves at Kalpakkam from remote forcing effects of Southern Ocean swells

Sashikant Nayak^a, Prasad K. Bhaskaran^{a,*}, R. Venkatesan^b, Sikha Dasgupta^b

^a Department of Ocean Engineering and Naval Architecture, Indian Institute of Technology Kharagpur, Kharagpur 721302, India

^b Radiological Safety Division, Indira Gandhi Centre for Atomic Research, Kalpakkam 603102, India

ARTICLE INFO

Article history:

Received 5 August 2012

Accepted 23 February 2013

Available online 15 March 2013

Keywords:

Wind-waves

Southern Ocean

Kalpakkam

Land-sea breeze

Swells

Wave spectrum

ABSTRACT

The importance of wave evolution and necessity for reliable prediction in coastal environments is widely recognized in many ocean engineering applications. Numerical wave models developed for limited area forecast can predict ocean waves fairly well upon imposing realistic boundary conditions from measurements. The forecast quality wherein depends on the number of measured data from various platforms specified along model boundary, which is undoubtedly very expensive. In a highly dynamic coastal environment, non-linear interaction from distant long period swells can essentially modulate the local wind-waves. This effect is more pronounced when local wind waves are opposed by distant swells reaching the coast. In addition, small scale convective phenomena like land and sea breeze create localized wind-sea having wide degree of directional behavior, thereby resulting in a more complex non-linear interaction process. For operational scenario, multi-scale modeling approach could be recommended as the best choice. The present work investigates influence of distant swells generated from Southern Ocean, and their role in modifying local wind-waves at coastal Kalpakkam located at south-east coast of India. Numerical experiments were performed to understand the influence of distant swells in modulating the local wind-waves which resulted in enhancing the wave energy by almost double off Kalpakkam coast.

© 2013 Elsevier Ltd. All rights reserved.

1. Introduction

The low frequency swells generated from Southern Ocean can travel thousands of kilometer crossing hemisphere and finally reaching coastal destinations of various continents. During their course of travel over long distances they mutually interact with locally generated wind waves thereby redistributing the overall wave energy. Observational reports from measurements conducted near Cape Town in South Africa (Shillington, 1981) points out the existence of unusual low frequency waves. Their study based on time series evaluation of one-dimensional wave energy from measurements revealed that these low frequency waves originated in the Southern Ocean, and traveled about 2800 nautical miles to the measurement location. The wave spectra analyzed from their study reveal quasi-regular swells of very low frequency, having spectral energy densities an order of magnitude larger than that occurred during normal conditions. This observational evidence brings to light the importance of remote modulation effects in association with locally generated wind-sea. Fig. 1 shows

propagation characteristics of swell waves from Southern Ocean basin toward the north Indian Ocean, where the contours marked as Days 1–4 depicts the movement of swell wave fronts, and the arrow represent the direction of swell propagation. As seen from this Fig. 1, the long distant swells generated from the Southern Ocean belt travel fast and reach the southern tip of Indian mainland in about 4 days with least dissipation.

Therefore, a comprehensive study on the remote modulation effects of distant swells to local wave climate has profound importance for a wide range of oceanographic studies and ocean engineering applications. Swell waves have longer wavelengths by virtue of which they refract at deeper waters offshore compared to local wind waves. The great circle propagation of global ocean swells has been a topic of interest in the past, and studies by Barber and Ursell (1948), Munk et al. (1963), Snodgrass et al. (1966) are notable. Thereafter, Donelan (1987), Chen and Belcher (2000) reported on how swell affects modulation, blockage and suppression of short period wind generated waves. More recently the role of swell propagation mechanisms which modify the atmospheric boundary layer has been reported by Chen et al. (2002), Ardhuin et al. (2003). A commonly used method to isolate swells from local wind-waves at a given location is called 'spectral partitioning' and a comprehensive review of existing techniques is reported by Hanson and Philips (2001).

* Corresponding author. Tel.: +91 3222 283772; fax: +91 3222 255303.

E-mail addresses: prasadlsu@yahoo.com,
pkbhaskaran@naval.iitkgp.ernet.in (P.K. Bhaskaran).

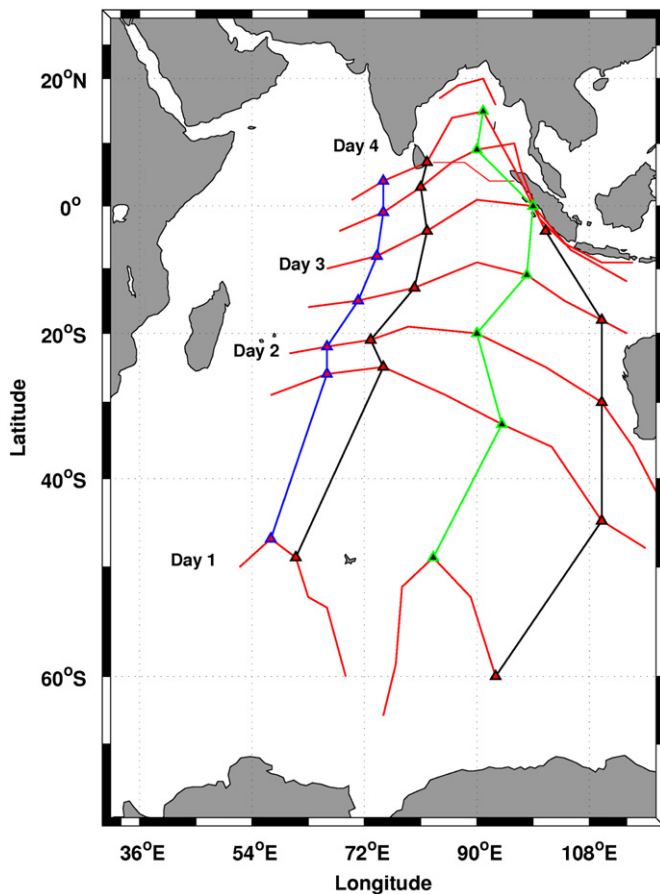


Fig. 1. Swell generation area in Southern Ocean and its advancement toward Indian mainland from possible directions.

As stated above, properties of long period swell waves are not significantly affected by surface wind stress as they move away from the generation area. The swells also undergo negligible energy loss due to viscous dissipation or white-capping mechanisms. In shallow and intermediate water depths swells are modified through refraction and bottom interaction process and their energy is totally dissipated at land boundaries. Hence their modulation with local wind-waves causing the redistribution of resultant wave energy at a given location should be essentially through the non-linear wave-wave interaction process, which is discussed in this study for a selected coastal location off Kalpakkam (Fig. 2) in the Bay of Bengal. Some interesting studies were also attempted earlier on swell dissipation affected by reverse momentum flux mechanism (Donelan et al., 1997; Grachev and Fairall, 2001; Smedman et al., 2003) which usually occurs as swells travel faster than the surface winds in most cases. There are also reports which state that the mechanism of wave turbulence interaction also leads to swell attenuation (Teixeira and Belcher, 2002). In this regard the energy transfer from wind-sea to swells is although a known process, the extent to which these contributions play their role in swell attenuation is still not known.

The hydrodynamic impact on the effect of remote modulation by swells on an inter-tidal estuarine mudflat in a near-shore area at San Francisco Bay was reported by Talke and Stacey (2003). Their study based on observational support points out that long period swells having time period between 10 and 20 s are the potential source of near-bed energy and stress in the near-shore shallow coastal zone. Many studies in the past were carried out in laboratory tanks and in

coastal areas to understand the growth of wind waves. In these experiments the fetch, an essential condition required for the waves to grow and evolve is fairly understood and well defined. In the open ocean, swells are known to travel over long distances with minimum attenuation and simultaneously interacting with the locally generated wind-waves. The resulting energy spectrum of ocean waves during this interaction process is not well understood. Mechanics of wave growth and evolution in a mixed sea state where both wind-sea and swells co-exist is a subject of interest from practical point of view. A recent study by Violante-Carvalho et al. (2004) shows the effect of long waves in modulating the energy of wind-sea by considering different propagation directions and frequencies of swells. A data set comprising of 5800 buoy observations from Campos basin located in the state of Rio de Janeiro were selected, and specific cases where direction of wind remained stable were used for analysis. The case of swell waves in their study was confined to shorter distances. In a recent study, the assessment of wave energy resources for Hawaii islands in the mid-Pacific was investigated by Stopa et al. (2011). The study revealed that Hawaii is subjected to direct approach of swells from distant storms. It brings to light that the localized wave field is modified by the far field swells. The study was based using state-of-art numerical models like Wave Watch III (WW3), Simulating Waves Near shore (SWAN) forced by winds from Weather Research and Forecast (WRF) model and NCEP Final Analysis (FNL). Their study highlights the importance of episodic swell events on wave energy resources around the Hawaii islands. Hence, based on the various studies described as above, it is evident that swells can modulate and significantly modify the local wave characteristics. In the presence of strong meso-scale phenomena like land-sea breeze in a coastal environment such as Kalpakkam region being investigated here can generate local wind-waves having a wide degree of directional behavior. The mixed sea-state resulting from this meso-scale phenomenon and by interacting with the long distant swells can lead into complex local wind-wave characteristics through their non-linear interaction process.

Long distant swells that originate from Southern Ocean can dynamically modulate and modify the wave climate in the near-shore areas. A multi-scale modeling approach was used, and thereby numerical experiments performed with and without the presence of long distant swells, that travel from Southern Ocean to the Kalpakkam coast. Numerical experiment was performed for the month of September 2008, when data for land-sea breeze event simulations from WRF model was available for this study from IGCAR, Kalpakkam. A high resolution unstructured version of SWAN model was used to study the influence of distant swells in modulating the local wind waves. The variance energy density spectrum from SWAN computations with and without the presence of swells was compared to understand the role of non-linear wave-wave interaction. The influence of distant swells are clearly visible and also significant in modulating the local wind-waves, wherein the resultant energy levels are seen to modify by almost double considering the background swell wave field.

2. Swell generation areas

In the North Indian Ocean swells are found both in the Arabian Sea and the Bay of Bengal. Swells dominate the west coast of India during the south-west as well as north-east monsoon seasons having occurrences of 93% and 67% respectively (Aboobacker et al., 2011). The pre-monsoon seasons are dominated by wind-sea. The predominant swells observed along the west coast of India during pre-monsoon and north-east monsoon seasons are from the south-west and south south-west directions, which

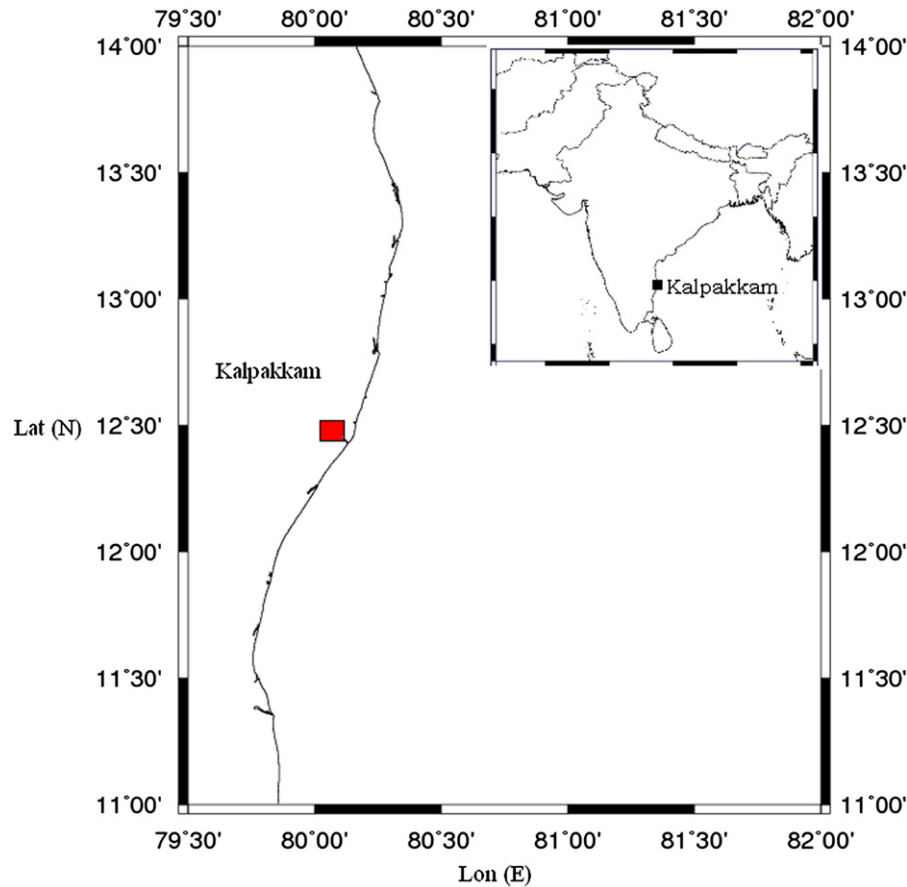


Fig. 2. Study area—location of Kalpakkam, south-east coast of India.

arrive from the south Indian Ocean. The predominant swells during the south-west monsoon season are generated in the north Indian Ocean. The potential generation areas of swells are: (i) area bounded by 52.5°E to 62.5°E and 5°S to 15°S for south-west swells during the south-west monsoon season, (ii) area bounded by 40°E to 70°E and 30°S to 50°S for south-west and south south-west swells during the pre-monsoon and north-east monsoon seasons, and (iii) area bounded by 60°E to 67.5°E and 17.5°N to 25°N for north-west swells during pre-monsoon and north-east monsoon seasons (Aboobacker et al., 2011). Another study by Alves (2006) revealed regarding three swell generation zones in the Indian Ocean viz; tropical north Indian Ocean, tropical south Indian Ocean and extra-tropical south Indian Ocean. It also points out that eastward propagating extra-tropical south Atlantic (ETSA) swell energy spreads through the entire Indian Ocean basin which reaches the coast of Thailand, Indonesia and south-western Australia extending up to the Tasman Sea. The ETSA swells are recognized as a significant component of the Indian Ocean affecting the wave climate in most part of the year (Alves, 2006). The distribution of wind-sea and swell wave data for the north Indian Ocean based on visual estimates from ships of opportunity and reported by India Meteorological Department (IMD) for the period from 1961–1970 is shown in Table 1 (Swain, 1997). As seen from this table, the numbers of swell events are more during the south-west monsoon period (May–September). The study by Swain (1997) for the north Indian Ocean indicates higher swell wave heights compared to wind-sea during both fair and rough weather seasons (north-east and south-west monsoon periods). The analysis of visually observed swells grouped in square grids of $1^\circ \times 1^\circ$ also revealed that swell

Table 1

Number of visually observed wind-sea and swell observations from IMD for the period 1961–1970 in the Indian Ocean.

S.No.	Month	Wind-sea	Swell
01	January	30,414	17,525
02	February	29,966	16,609
03	March	29,005	17,245
04	April	24,767	17,829
05	May	33,988	23,086
06	June	36,683	24,894
07	July	37,253	25,617
08	August	37,596	26,163
09	September	31,266	22,243
10	October	26,978	19,574
11	November	27,576	18,258
12	December	30,523	18,139
Total		379,015	247,182

heights are higher compared to wind-sea with due consideration that there is intrinsic human error on visually based estimates. By and large it is well known that the swells do influence by modulating the local wind-sea. However, a comprehensive study on how they interact with the wind-seas and transfer energy during wave evolution in terms of its quantification and energy redistribution for the Indian Ocean has not been reported so far. Therefore, the authors believe that, understanding of this non-linear wave-wave interaction process and its quantification at selected locations can help in better understanding of the role of modulation effects on local wind-seas in coastal areas.

3. Study location—off Kalpakkam coast, Bay of Bengal

Kalpakkam is a small coastal town situated in the Coromandel coast approximately 70 km south of Chennai, a metropolis located in the South India. The topographic characteristic of Kalpakkam is a gentle sloping plain terrain, where the temperature over the land is relatively high. The contrasting temperature differences between land and sea along with large scale geostrophic winds favorable for the occurrence of sea breeze. During mid-summer, the temperature gradient between land and the sea can be significantly higher. In Chennai (north of Kalpakkam), the maximum temperature over land is about 42 °C whereas the SST is about 27 °C. Such contrasting temperature can lead to stronger sea breeze, which can also oppose the geostrophic wind. The location of Kalpakkam being in the tropical belt (closer to the equator) experiences weak Coriolis force conducive for steering the wind system deep inland. Studies based on micro-meteorological experiments to study the structure of atmospheric boundary layer during sea breeze events around Kalpakkam was reported by Thara et al. (2002), Sivaramakrishnan and Venkatesan (2002).

The study region off Kalpakkam covers an area about 40,000 km² (domain 'D3' in Fig. 3) encompassing the Kalpakkam nuclear plant, which is of strategic importance located between 12° 30' N latitude and 80° 10' E longitude, east coast of India. The coastline is nearly straight and oriented in the Northeast–Southwest direction. Coastal Kalpakkam is about 5 m above Mean Sea Level (MSL) which increases gradually up to 100 m above MSL approximately 100 km across the coast. The site comprises of dedicated meso-observational network of

meteorological towers located very close to the coast, and Anupuram field experimental site about 5 km onshore the coast.

4. Methodology

A multi-scale nested approach was used to simulate the non-linear interaction effects due to distinct swell wave systems (Fig. 1) in the coastal region off Kalpakkam (Fig. 3). To do so, three different model domains were used to predict the influence of long swells reaching the coastal destination as shown in Fig. 3. The outer domain (D1) is a finite difference coarse grid extending up to 70°S, and numerical experiment was performed using the latest version of WAM-Cycle 4.5.3, the state-of-art third generation wave prediction model (Gunther and Behrens, 2011). The boundary conditions containing information of two-dimensional wave energy spectra from coarse grid (domain D1) was nested to the intermediate finite difference grid domain (D2) which is then subsequently nested to the inner domain (D3) which is the region of study considering a fine resolution finite element grid system. For the prediction of waves in coastal, near-shore and estuarine waters, models like SWAN (Booij et al., 1999) is well known owing to advanced model physics dealt approximately for the shallow water environment. Hence, SWAN model was used to predict wave characteristics in domains D2 and D3 by utilizing boundary conditions from D1. Two separate experiments have been attempted to assess the influence of long swells reaching the inner domain (D3). In the first experiment, all three domains (D1, D2 and D3) were taken into consideration, whereas in the second experiment only the domains D2 and D3 were considered which essentially cut-off the propagation of swells from Southern Ocean. In coastal and near-shore waters, the need of a high resolution atmospheric model capable of simulating small scale features such as land and sea breeze is an essential pre-requisite for wave prediction purposes. An earlier study indicates that WRF model configured for the Kalpakkam region had demonstrated its robustness to simulate land and sea breeze events fairly well. Therefore, WRF (Weather Research and Forecast) wind fields were considered as the best choice of input fields for SWAN model in domain D3 with an aim to simulate near shore wave dynamics and the non-interaction process due to the advection of swell waves into the region of locally generated complex wind-seas driven by alternating land–sea breeze.

4.1. The wave models

WAM cycle 4.5.3 is the updated version of WAM cycle-4 wave model described in Komen et al. (1994) and Gunther et al. (1992). The basic physics and numerical approaches of wave evolution in space and time can be found in the report of Komen et al. (1994). WAM 4.5.3 incorporates the source function integration scheme proposed by Hersbach and Janssen (1999) and Bidlot et al. (2005) which is a new semi-implicit method developed at ECMWF. It is expressed in the form

$$F_{n+1} = F_n + \frac{\Delta t S}{1 - \Delta t G} \quad (1)$$

where $S = S(u_{n+1}, F_n)$ is the source function of spectrum computed at time (n) and wind speed (u) at time level ($n+1$). The term ' G ' in the above equation is given by $G = G(u_{n+1}, F_n)$. The other developments in version 4.5.3 attributes to the dissipation source function expressed in terms of mean steepness and specification of mean frequency giving more importance to the high frequency part of the wave spectrum. These new additions in version 4.5.3 provide a more realistic interaction between wind-sea and swell waves. The other improvement is with reference to the time-stepping algorithm which allows propagation time step to be longer than

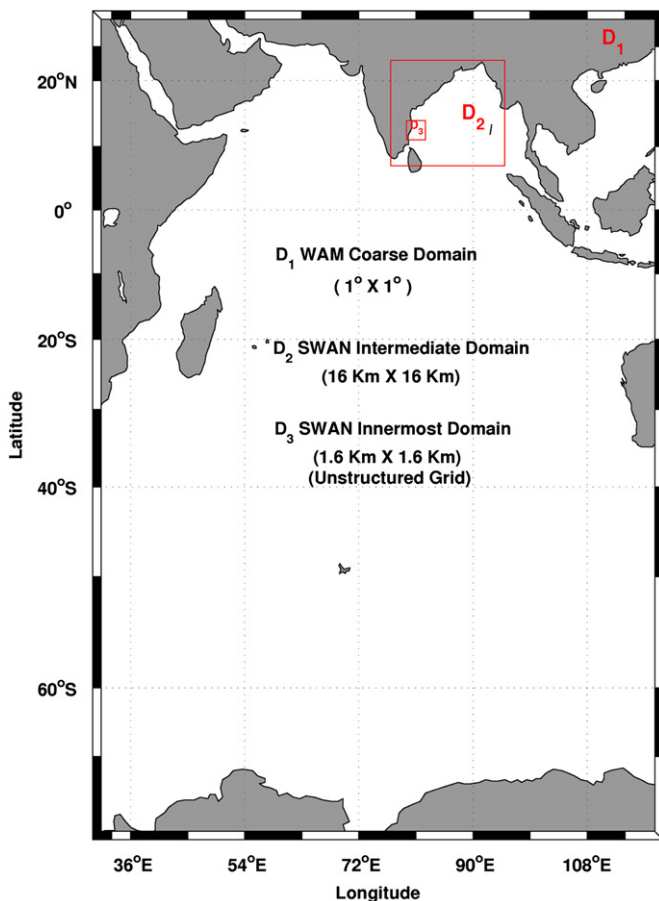


Fig. 3. Multi-scale model domains for the numerical experiment (D1—coarse grid WAM domain; D2—intermediate finite difference grid; and D3—unstructured finite element fine grid SWAN domain).

source function time step. The advantage being computational speed is boosted for very high spatial resolutions. For more details of WAM 4.5.3 may be seen from [Gunther and Behrens \(2011\)](#).

The evolution of SWAN wave spectrum in a cartesian coordinate system can be described by the spectral action balance equation expressed in the form

$$\frac{\partial N}{\partial t} + \frac{\partial}{\partial x} c_x N + \frac{\partial}{\partial y} c_y N + \frac{\partial}{\partial \sigma} c_\sigma N + \frac{\partial}{\partial \theta} c_\theta N = \frac{S}{\sigma} \quad (2)$$

The terms in Eq. (2) are the relative frequency (σ), wave direction (θ), the wave action density (N), the ratio of spectral energy density with intrinsic frequency. In mathematical sense, $N(\sigma, \theta) = E(\sigma, \theta)/\sigma$ where $E(\sigma, \theta)$ is the wave energy density. In this equation the first term on the left hand side (LHS) represents the local rate of change of action density with time. The second and third terms represent geographic propagation of action density with propagation velocities ' c_x ' and ' c_y ' in the X–Y space respectively. The fourth term represents shifting of relative frequency arising due to variation in bathymetry and currents with propagation velocity ' c_σ ' in the ' σ ' space. The fifth term accounts for depth and current induced refraction of propagation velocity ' c_θ ' in the ' θ ' space. In the right hand side (RHS) of Eq. (2) the term ' S ' is cumulative sum of the action balance equation which is sum of various source and sink mechanisms which is a function of wave energy density. The various source/sink mechanisms includes: wind-input (momentum transfer from atmosphere to ocean), non-linear wave–wave interaction, white capping dissipation and bottom interaction (for shallow waters).

The physical parameterization of various source/sink terms in SWAN model is superior to WAM 4.5.3 model. This makes SWAN more flexible through optional switches enabling the user to select the appropriate model physics for the region of interest. The integration of the action balance equation is implemented in the SWAN model with finite difference schemes in all five dimensions which includes time (t), geographic space (x, y) and spectral space (σ, θ). The finite difference form can be expressed as follows:

$$\begin{aligned} & \left[\frac{N^{i_t, n} - N^{i_t-1, n}}{\Delta t} \right]_{i_x, i_y, i_\sigma, i_\theta} + \left[\frac{(c_x N)_{i_x} - (c_x N)_{i_x-1}}{\Delta x} \right]_{i_x, i_y, i_\sigma, i_\theta}^{i_t, n} \\ & + \left[\frac{(c_y N)_{i_y} - (c_y N)_{i_y-1}}{\Delta y} \right]_{i_x, i_y, i_\sigma, i_\theta}^{i_t, n} \\ & + \left[\frac{(1-nu)(c_\sigma N)_{i_\sigma+1} + 2nu(c_\sigma N) - (1+nu)(c_\sigma N)_{i_\sigma-1}}{2\Delta\sigma} \right]_{i_x, i_y, i_\sigma, i_\theta}^{i_t, n} \\ & + \left[\frac{(1-nv)(c_\theta N)_{i_\theta+1} + 2nv(c_\theta N)_{i_\theta} - (1+nv)(c_\theta N)_{i_\theta-1}}{2\Delta\theta} \right]_{i_x, i_y, i_\sigma, i_\theta}^{i_t, n} \\ & = \left[\frac{S}{\sigma} \right]_{i_x, i_y, i_\sigma, i_\theta}^{i_t, n*} \end{aligned} \quad (3)$$

In Eq. (3), Δt is the propagation time step; Δx , Δy , $\Delta \sigma$ and $\Delta \theta$ are increments in geographic space and spectral space respectively. The symbol ' i_t ' represents the time-level index; i_x , i_y , i_σ , and i_θ are the grid counters, n^* is equal to ' n ' or ' $n-1$ ' for explicit or implicit approximations depending on the source term with ' n ' being the number of iterations. The coefficients ' nu ' and ' nv ' determine the degree to which the scheme is upwind or central in spectral space. They control the numerical diffusion in frequency and direction space. The SWAN model used in the present study is most suitable to study the non-linear interaction process between distant swells and locally generated wind waves. The physics of triad non-linear interaction process which utilizes the Lumped Triad approximation (LTA) theory in SWAN model was used to investigate the influence of long swells and its role in modifying the local wind-waves off Kalpakkam.

4.2. Input wind fields for the wave models

The input winds used in the present study for the outer domain (D1) and intermediate domain (D2) is the blended ECMWF winds available for the global oceans. Strong winds above 20 ms^{-1} prevails in the Southern Ocean south of 50°S , which is a potential area for swell generation. The blending algorithm utilizes remotely sensed retrievals in the ECMWF analysis which enhances the quality of the wind product. The temporal and spatial resolution of data used in this study are the six hourly zonal and meridional components of surface wind fields over $0.25^\circ \times 0.25^\circ$. Remotely sensed wind observations derived from scatterometer onboard QuikSCAT, SSM/I onboard DMSP satellites were used for preparation of the analyzed ECMWF wind products. These blended winds had undergone thorough quality checks with marine observations and their correlation coefficients have ranged from 0.80 to 0.90 for the global oceans. As wave models are very sensitive to input wind forcing, based on the skill scores of blended ECMWF products, it is ascertained that best quality wind fields were used in this study. Details on the computational algorithm may be found in [Bentamy et al. \(2007\)](#).

4.3. Land and sea breezes off Kalpakkam coast

The alternating land and sea breezes near coastal areas is a meso-scale phenomenon having direct bearing on the local weather. A precise knowledge of this meso-scale phenomenon has wide practical applications such as air pollution dispersion, sailing and surfing activities, and many more. In most coastal areas worldwide, there have been numerous attempts in the past to understand its strength and directional behavior. An experimental base to study its characteristics was reported by [Ogawa et al. \(1986\)](#), [Osamu et al. \(1994\)](#), [Melas et al. \(1995\)](#). Some notable theoretical work on land-sea breezes having implications on dispersion characteristics of air pollutants was investigated by [Gross \(1986\)](#), [Xian and Peilke \(1991\)](#), [Cai and Steyn \(2000\)](#), [Liu et al. \(2001\)](#). In the context of coastal Kalpakkam, simulations of land-sea breeze events have been studied in the past, but with different objectives. There were various studies conducted at coastal Kalpakkam related to atmospheric dispersion of radio nuclides emanating from the nuclear plant using Gaussian dispersion model integrated with a sea breeze meso-scale model ([Venkatesan et al., 2002](#)). Sensitivity studies of the meso-scale land-sea breeze model for coastal Kalpakkam for radio nuclide dispersion and influence of boundary layer turbulence parameterization was reported by [Srinivas and Venkatesan \(2005\)](#) and [Srinivas et al. \(2007\)](#). Therefore it could be noted from these studies that more emphasis was laid on atmospheric dispersion modeling and less on coastal oceanographic processes. The WRF model configured for the coastal Kalpakkam had proved its robustness in simulating land-sea breeze phenomena relatively well. Hence in our present study, the surface wind field obtained from WRF model for the period of September 2008 was used to force SWAN model for the inner domain D3.

4.3.1. Simulation with WRF model

The Weather Research and Forecast (WRF) model is a sophisticated Numerical Weather Prediction (NWP) model that solves the compressible non-hydrostatic Euler equations in a flux form, on a mass based terrain following vertical coordinate system. Prognostic variables from this model includes the horizontal and vertical wind components, various microphysical quantities, perturbation potential temperature, geopotential height and surface pressure of dry air. It is a fully compressible non-hydrostatic model. The model uses the Runge-Kutta 3rd order time integration scheme and the 2nd to 6th order advection schemes in both horizontal and vertical directions.

A complete description of the WRF modeling system is reported by Skamarock et al. (2005).

For the present study, single domain of integration is used in the model. The vertical resolution has 28 ETA levels and a horizontal mesh of 2 km coverage encompass the Kalpakkam region. The horizontal domain of integration was 360 km \times 360 km. To capture the effects of land and sea breeze events in the simulation, part of land and sea has been included in the domain. A detailed description of the grids and model physics options used in WRF are shown in Table 2. The initial and boundary conditions for WRF are provided from NCEP global 1° \times 1° resolution final analysis (FNL) data. This contains horizontal and vertical winds, sea level pressure, surface pressure, temperature, sea surface temperature, geopotential height, etc. The model was initialized at '0000 Z' Indian Standard Time (IST) of 1st September 2008 and integrated for 30 days. The lateral and boundary condition in the model are updated at every 6-h interval. The surface temperature of land was predicted by a land surface scheme included in the model. The surface boundary values for terrain height, albedo, moisture availability, emissivity, roughness coefficient, etc. are specified from USGS data and interpolated to the model grids. The atmospheric radiation and cooling rates are calculated at intervals of every 30 min.

4.4. Model initialization procedure

The primary inputs are an essential pre-requisite to model the evolution of surface gravity waves viz; time varying wind field, surface current, water level variations and bottom topography. The bathymetry data for the study region covering the north Indian Ocean and Southern Ocean (30°N–70°S; 30°E–120°E) was extracted from the global ETOPO1 database of 1° \times 1° grid resolution. Two sets of numerical experiments were performed using the multi-modeling approach to investigate the behavior of wave evolution at Kalpakkam. These experiments were performed using multiple nesting of model runs, wherein the boundary information of two-dimensional wave energy spectra was provided by WAM 4.5.3 as input to subsequent SWAN nested runs. The lateral boundary information for the inner domain (D3) of SWAN is the region of interest to study modulation effects due to distant swells. A bilinear interpolation procedure was executed in the final preparation of bathymetric database for the inner domain (D3) by blending the actual survey records of bathymetry conducted for the Kalpakkam region. Finite difference grids were used for the computation of wave parameters in both the outer (D1) and intermediate domains (D2), whereas the high resolution finite element grid was used for reliable wave computations in the inner domain (D3) off Kalpakkam. The frequency and angular discretization prescribed for the SWAN model runs in the inner domains was 49 and 50 respectively, and this should capture the entire spectrum of surface waves with a

higher precision of frequency and angular distribution, notably the swell components. The resultant time varying two dimensional energy spectrum was investigated for two deep water points (Locations 21 and 22), and at a coastal Location-1 (Fig. 4) where the water depth is about 33 m and having a mild beach slope. The deep water locations (21 and 22) were chosen along the boundary of the high resolution finite element mesh, which were the possible path ways that swells propagated to the Tamil Nadu coast.

5. Results and discussion

The land–sea breeze phenomena which prevailed off Kalpakkam coast are shown in Fig. 5. As seen the variability of wind field with reference to Kalpakkam location can be categorized into three groups viz; parallel to the coast (P), land breeze (LB) and sea breeze (SB). Fig. 5a shows the occurrence of sea breeze event for a period of 2 days (1st and 2nd September), whereas the next 3 days until 05 September was dominated by winds parallel to the coast. From 5 to 10 September the prominence of land breeze event was noticed. The winds parallel to the coast and the predominance of land breeze events are found during 6–29 September, wherein the occurrence of sea breeze condition was insignificant (Fig. 5b and c). The winds parallel to the coast as shown in Fig. 5b and c where alternatively followed by land breeze events. By and large, the near-shore wind events were land breeze during 6–29 September. A composite picture for the overall monthly wind distribution also ascertains that the dominant activity which persisted along Kalpakkam coast during September 2008 was land breeze followed by intermittent occurrences of winds parallel to the coast. The overall situation was not conducive for sea breeze events. To quantify the monthly near-shore wind scenario, it can be pointed out that 39% of occurrences are the winds parallel to coast, 6% are sea breeze events and remaining 55% corresponds to land breeze events.

The analysis of surface wind fields from blended ECMWF data shows that around first week of September 2008 (Fig. 6) south-west winds prevailed over Arabian Sea with magnitude of approximately 10 ms^{−1}. However, in the Bay of Bengal, predominant winds were south-easterly with magnitudes ranging from 4 to 6 ms^{−1}. Easterly winds prevailed in the equatorial Indian Ocean having similar wind strength as in the Arabian Sea. The winds were stronger around 10°S and the prevalent wind direction was south-east. Overall winds were further strong in the Southern Ocean with magnitudes in excess of 12 ms^{−1}. Along the eastern and western boundary of southern Indian Ocean the winds ranged from 18 to 20 ms^{−1}. A notable feature in the Southern Ocean is the existence of fast moving synoptic storms from west to the east. During the middle of September, 2008 the western Arabian Sea experienced persistent south-west winds with magnitudes ranging between 9 and 12 ms^{−1} off Somalia coast and also in central Arabian Sea. The overall wind speeds were higher in the central Bay of Bengal up to 15 ms^{−1} with weaker winds persisting all along the equatorial Indian Ocean. The Southern Ocean continued to have strong winds with magnitudes in excess of 27 ms^{−1} due to sporadic storms. The rapid migration of synoptic storms toward east was noticed in the Southern Ocean until end September 2008. In general, the wind system in the Southern Ocean was found to be persistently high compared to rest of the outer model domain (D1). These strong winds with unlimited fetch are undoubtedly the potential source of long distant swells propagating into the study region. The inner domain (D3) uses the WRF simulated wind field customized for the Kalpakkam region (Fig. 7) and obtained from IGCAR, Kalpakkam.

The variation of significant wave heights (in meters) at coastal Kalpakkam (Location-1, Fig. 4) with and without considering the swell propagation from Southern Ocean are shown in Fig. 8.

Table 2
Details of the grids and model physics used in the WRF model.

Dynamics	Non-hydrostatic
Vertical resolution	28 ETA levels
Horizontal resolution	2 km
Domain of integration	360 km \times 360 km
Radiation	Dudhia scheme for short wave radiation, Rapid Radiation Transfer Model (RRTM) for long wave radiation
Surface processes	NOAA land surface model
Planetary boundary layer	Mellor–Yamada–Janjic (MYJ)
Explicit moisture	WSM 3 class simple ice scheme

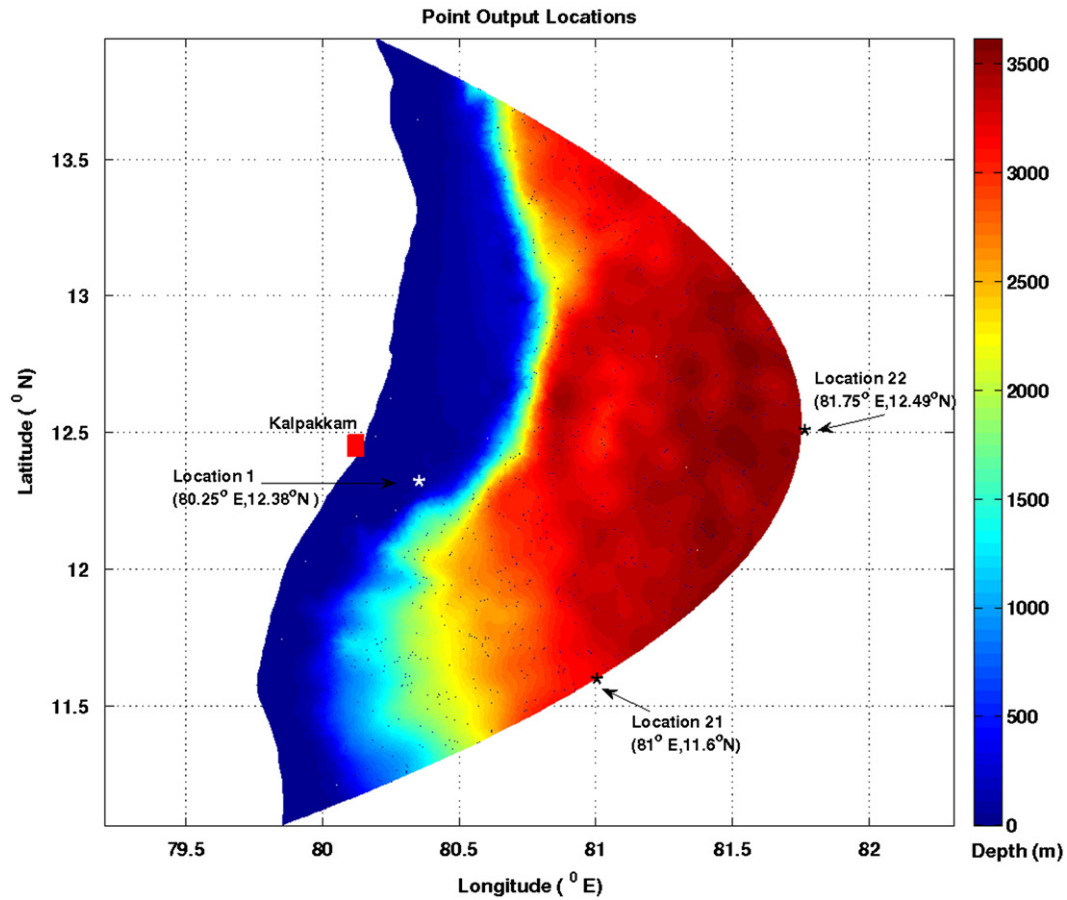


Fig. 4. Reference locations along the boundary (locations 21 and 22) and inner domain (location-1) of fine grid SWAN to evaluate influence of long swells off Kalpakkam.

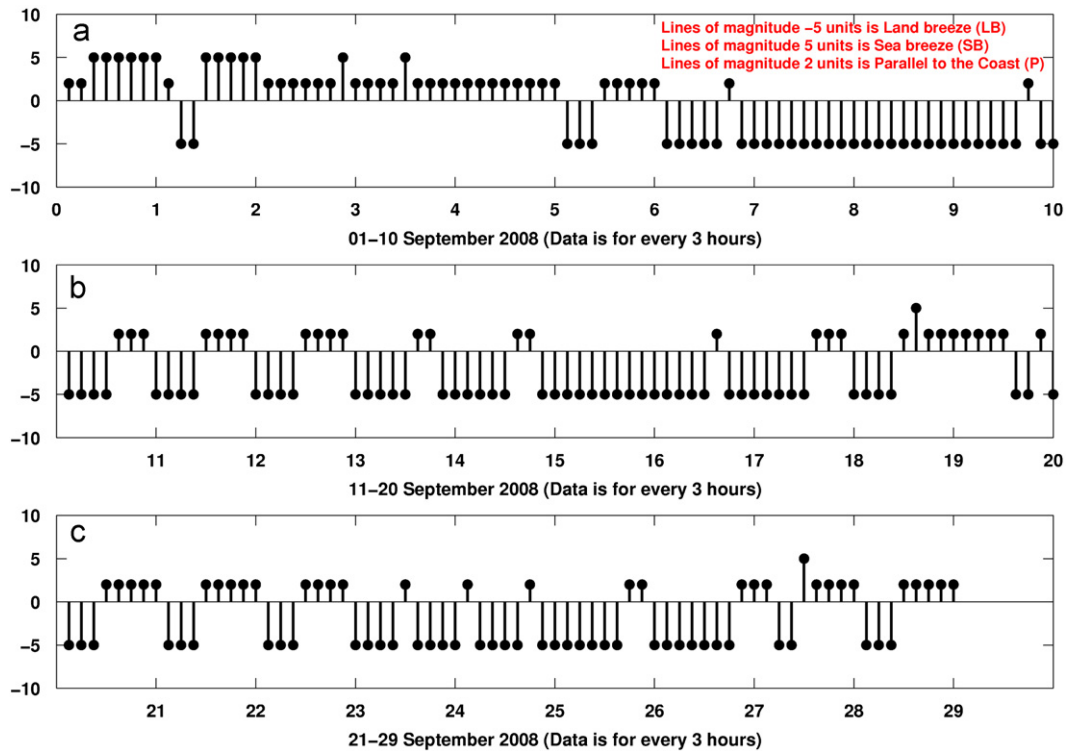


Fig. 5. Classification of Land Breeze (LB), Sea Breeze (SB) and wind system parallel to coast (P) off Kalpakkam during the period 01–29 September, 2008 as simulated by WRF model.

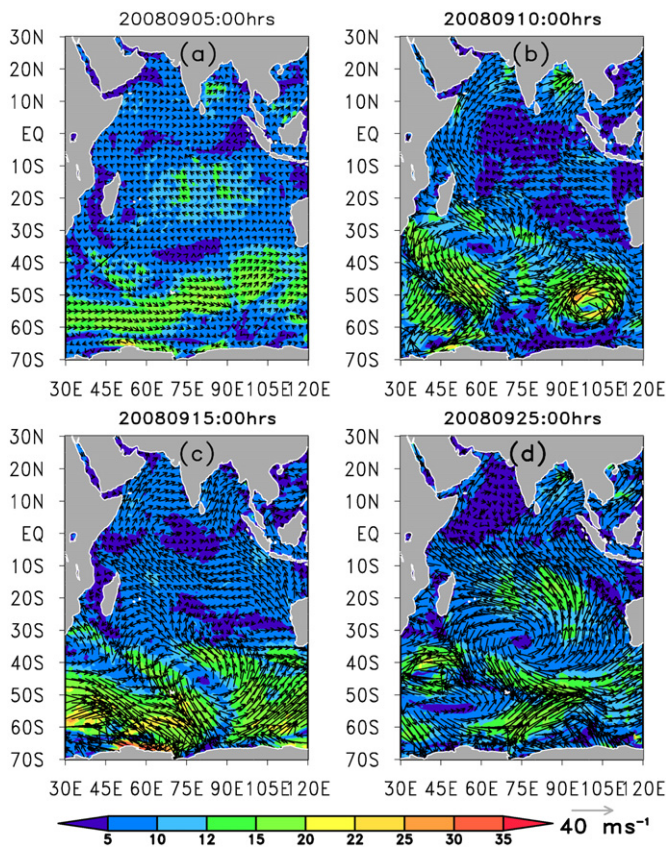


Fig. 6. Blended ECMWF wind field (a–d) for coarse grid WAM run and intermediate grid of SWAN run.

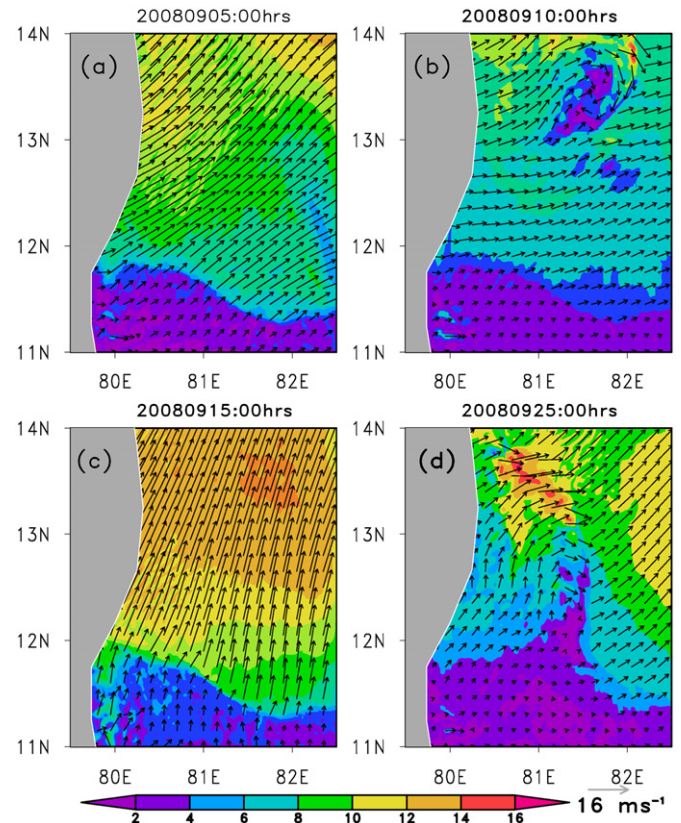


Fig. 7. WRF wind field for inner domain SWAN run.

During the first half of September 2008, the significant wave height was less than 1.5 m both in the Arabian Sea and Bay of Bengal with mean wave periods ranging between 5 and 6 s. The regions off Somalia and off Sri Lanka in the north Indian Ocean experienced relatively higher significant wave heights. During this period, significant wave height greater than 2 m prevailed over the Southern Ocean. The mean wave periods over Southern Ocean were > 8 s during September 2008. However, the mean wave periods during the synoptic storm events were ≈ 14 s. The region of high wave periods (≈ 14 s) was in Southern Ocean around 105°E (05 September, 18 h). Estimated forward speed of synoptic storms, taking into consideration the core movement was approximately 135 km h^{-1} . The overall wave period in Southern Ocean basin was higher than 10 s. The propagation of waves with high wave periods toward the equatorial belt resulted in an overall increase of wave periods both in the Arabian Sea and Bay of Bengal regions. During September, 2008 higher wave periods (> 12 s) are noticed along the eastward limit of Southern Ocean basin, as well in the north Indian Ocean. During this time the southern tip of Indian mainland experienced swells of period > 10 s. The mean wave periods in both the Arabian Sea and Bay of Bengal ranged between 8 and 10 s. In the last quarter of September (around 20 September) long period waves (> 14 s) were found in regions close to west Australia. Those waves on their arrival in Western Australia retroflex, a part travels toward the Java and Sumatra basin and remaining move in north-west direction reaching the north Indian Ocean basin. Toward end of 29 September, mean wave periods > 12 s are noticed both in the Arabian Sea and Bay of Bengal. It may be seen that the swell waves generated in the Southern Ocean migrate eastward and on reaching the western Australia spread out and propagate in the north-west

direction and reach the north Indian Ocean. Due to this, the mean wave periods are seen to be increased in both the Arabian Sea and Bay of Bengal regions.

The results clearly indicate that, the wave system at coastal Kalpakkam are being modulated by the modulation mechanism (Fig. 8). It may be noted that, the mean significant wave height (Fig. 8) is about 0.7 m when modulation effects of Southern Ocean swells are cut-off. Whereas, by considering the swell effects it modulates the local wind-sea off Kalpakkam with mean significant wave height around 1.3 m. It reveals that, the long period swells generated due to high wave activity in the Southern Ocean directly contributes toward higher wave activity in the study region in the Bay of Bengal. This brings to light that the higher wave activity in the Southern Oceans has a direct bearing on the wave climate which prevails in the Bay of Bengal.

5.1. Role of non-linear wave–wave interaction

The energy transfer among wave components due to nonlinear interactions was considered an important aspect for determining the evolution of the wave directional spectrum since the pioneering JONSWAP experiment in the North Sea. A possible mechanism by which wave energy can be transferred from one wave system to another is through resonant non-linear wave–wave interaction. The non-linear interaction process involving resonance among groups of four wave components was earlier demonstrated to play a key role in the evolution of wave spectrum in fetch limited situation (Hasselmann et al., 1973). The quadruplet wave–wave interaction based on discrete interaction approximation (DIA) theory is valid for deep waters. In shallow and coastal seas the Lumped Triad Approximation (LTA) theory reducing the quadruplets to triads is valid. In the present study, the deep water model

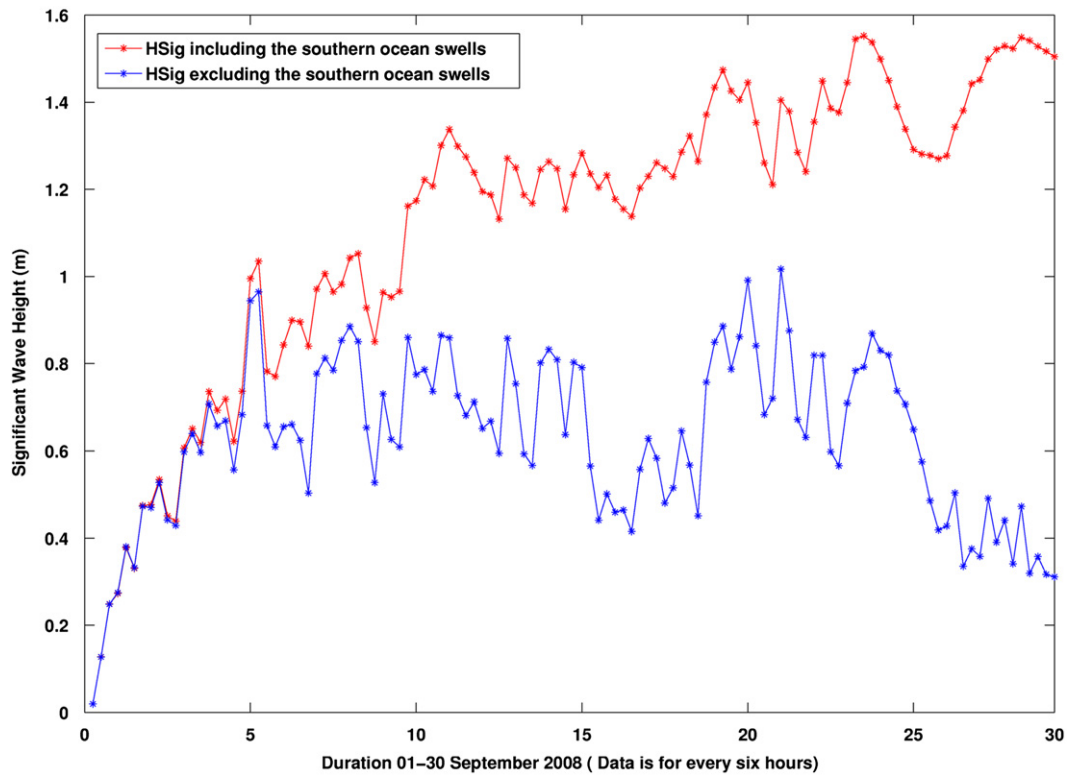


Fig. 8. Temporal distribution of significant wave height at location-1 (in meters) using multi-scale model domains.

runs using WAM4.5.3 were performed using quadruplets, and near-shore wave model run using SWAN was performed using the triad wave-wave interaction. In a given sea-state where wind waves develop in the presence of swells, the resultant wave field is comprised of two wave systems which can be described in the frequency-direction space by a bimodal spectral distribution. To investigate the role of background swells on local wind-sea two discrete locations were identified along the lateral boundary of the inner model domain (D3). The locations corresponding to 21 and 22 marked in Fig. 4 were used to assess the role of swells in modulating the local wind-sea. The Figs. 9 and 10 represent the temporal variation of frequency-direction integrated energy distribution due to non-linear wave-wave interaction (quadruplets) at locations 21 and 22 respectively during the month of September 2008. As noticed from both these plots, the non-linear energy transfer due to distant swell interaction is noticed from sixth day at these locations as the model appears to be satisfied from 5th day of its execution. The resultant energy build up due to the non-linear transfer process and the swells which propagate independently on an average is about 70% higher considering the distant swells. In other words, the swells have modulated the local wind-sea resulting in higher sea-state conditions.

5.2. Variance density spectrum

The importance of spectral peaks and their close transformation in the frequency-direction space based on numerical experiments were demonstrated by Young et al. (1995) and Mason (1993). The exact calculation of the energy transfer due to non-linear interaction process is quite complicated and computationally very intensive. An attempt to study the energy transfer process and its dependence on directional spread was carried out by Lavrenov and Ocampo-Torres, 1999. The temporal variation of variance density spectrum computed at Location-1 with

and without consideration of background swell are shown in Figs. 11 and 12. An overall comparison between these two plots, show that the relative energy levels due to background swells in the near-shore area off Kalpakkam is almost double. The maximum variance density at Location-1 ignoring swell effect was $0.45 \text{ m}^2 \text{ Hz}^{-1}$, which results to $0.95 \text{ m}^2 \text{ Hz}^{-1}$ by considering the distant swells into the study area. During the period 18 to 25 September 2008 higher values of variance density are observed in Fig. 12 compared to Fig. 11. During this period the wind field in the outer domain (D1) from blended ECMWF was found orienting from northerly to almost north-westerly. The prevailing wind direction was favorable for distant swells to approach the coastal belt in the near vicinity off Kalpakkam. During this period the local wind system off Kalpakkam is parallel to the coast prior to the land breeze event as evidenced from WRF winds in the inner domain (D3). Thereafter, the core of maximum variance density can be seen migrating toward low frequency. This is clearly distinct in Fig. 12, unlike the case in Fig. 11. It basically means that swells by virtue of modulating the local wind-sea also simultaneously result in transforming the short period waves to longer waves. The time-series distribution of variance density spectrum as seen from Fig. 12 appears to be a mutually decoupled, wherein distinct high energy patches at different frequencies are separated. The overall energy distribution in between these frequencies associated with high energy levels is quite low and this seems to be practically unrealistic. This is unlike the case noticed in Fig. 11 where the re-distribution of variance density due to non-linear wave-wave interaction is almost evenly spread in frequencies ranging from 0.05 Hz to 0.21 Hz. The results of these numerical study locations reveal the fact that energy transfer by considering individual waves components in a spectra comprising of wind-sea and swells is less than that when considering the combined wind-sea and swell in one bi-modal spectrum. In terms of the influence of distant swells

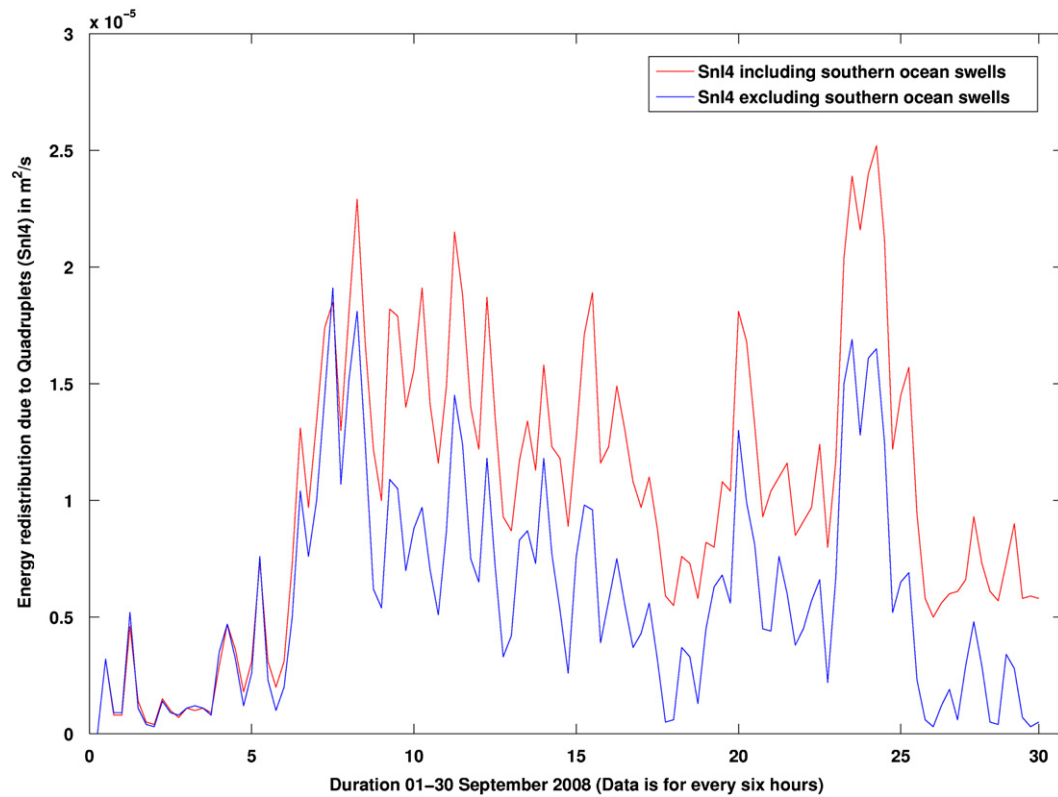


Fig. 9. Integrated frequency dependent energy distribution ($\text{m}^2 \text{s}^{-1}$) contributed through non-linear wave-wave interaction process at location-21.

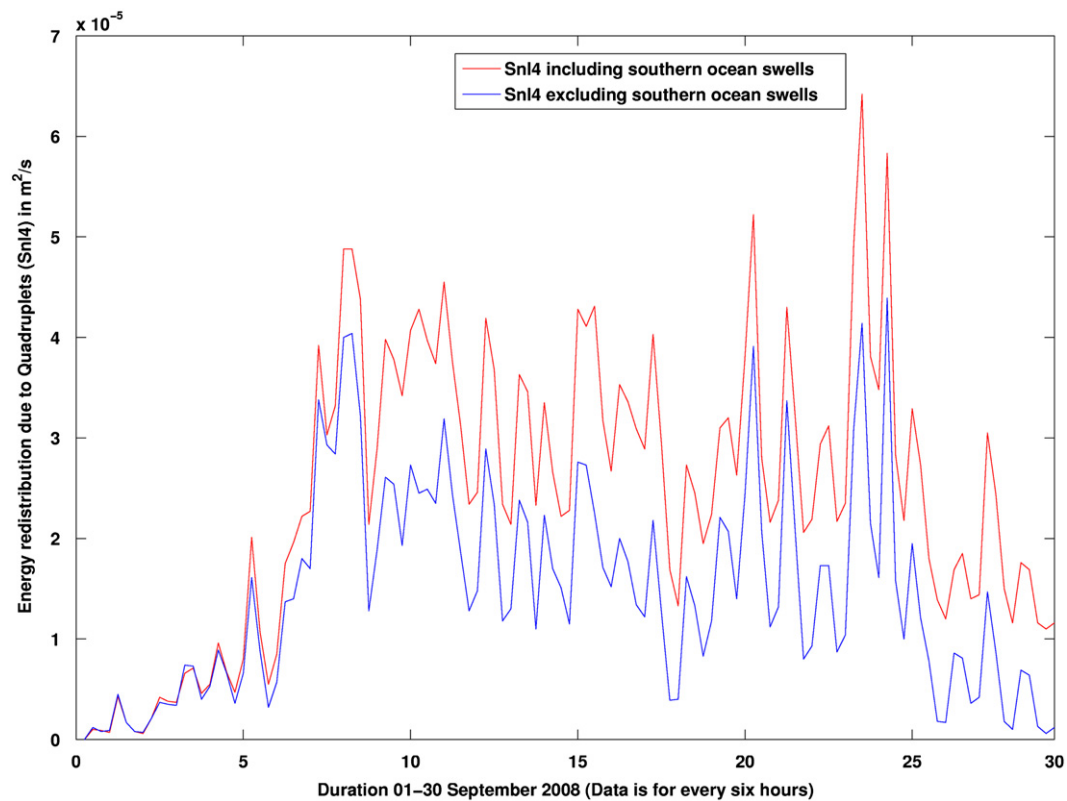


Fig. 10. Integrated frequency dependent energy distribution ($\text{m}^2 \text{s}^{-1}$) contributed through non-linear wave-wave interaction process at location-22.

on local wind-sea the relative nonlinear energy transfer process is greater for a wide frequency spectrum. This in turn can affect the spectral behavior by taking into account the combined wind-sea

and swells as one entity. The results in our findings are in close conjunction with the proposition and a recent study by [Violante-Carvalho et al. \(2004\)](#) where the buoy observations were used to

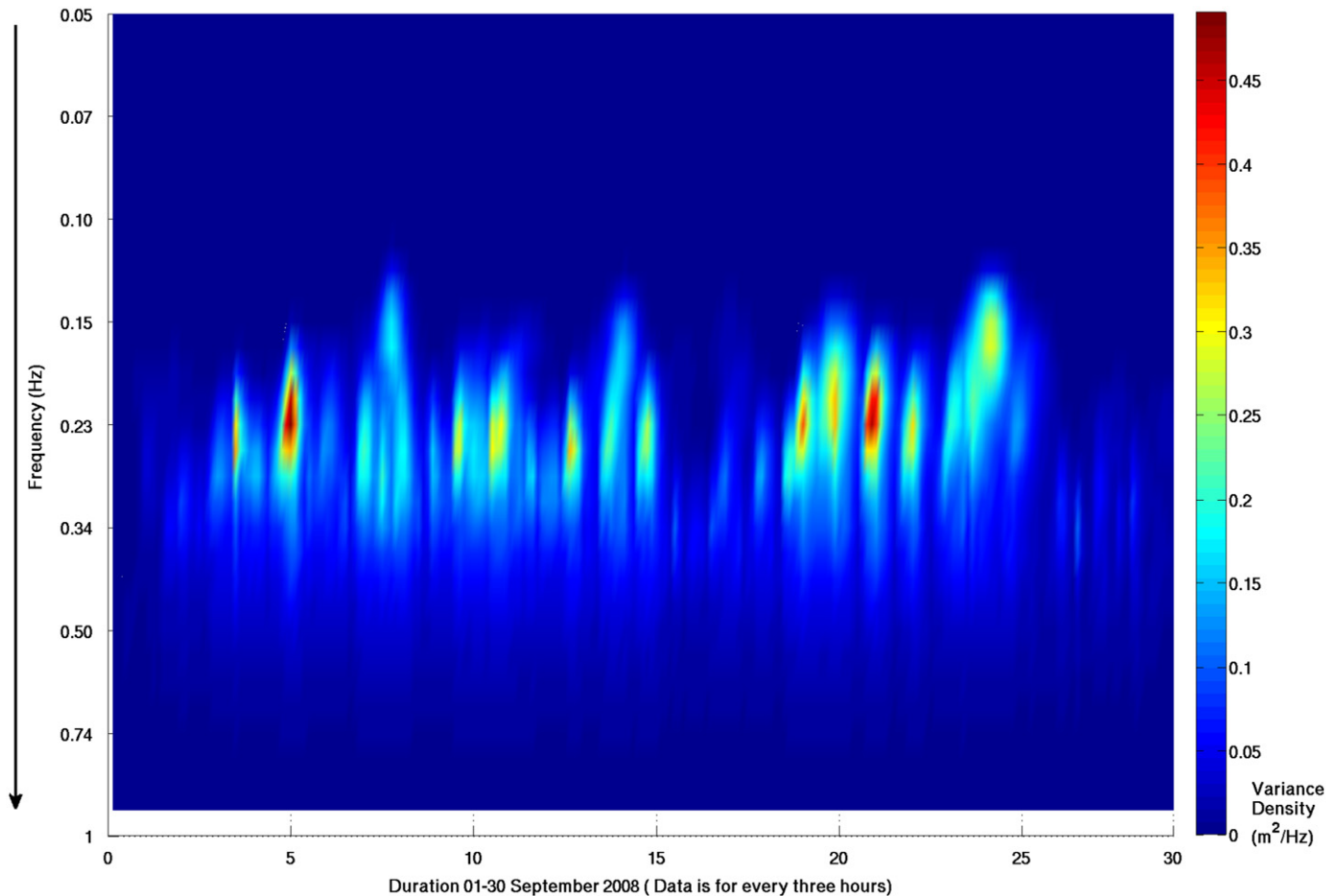


Fig. 11. Evolution of wave variance density spectrum ($\text{m}^2 \text{Hz}^{-1}$) during September 2008 at location-1 without considering the effect of long swells from Southern Ocean.

study the influence of swells on wind-waves in the open ocean. This deciphers the fact that nonlinear wave–wave interaction process taking into account contributions from distant swells can add energy to the resultant wave system in a fully developed sea, notably potential for an operational wave forecasting system.

6. Summary and conclusions

The work reports on a multi-scale modeling approach to understand the role of distant swells and their effects in modifying the sea-state in the presence of locally generated wind waves. Two sets of numerical experiments were performed to assess the resulting variation of variance density at a coastal destination in the close vicinity of Kalpakkam, located in the south-east Tamil Nadu coast, India. The numerical experiments in multi-scale approach was performed by closing the lateral boundaries in a manner to allow/prevent the presence of long distant swells which propagate from the Southern Ocean to the study area. Hence outer, intermediate and inner model domains were defined to quantify the nonlinear interaction process on the influence of swells on wind-waves off Kalpakkam. The numerical experiment was performed for the month of September 2008 and the resulting temporal variation of variation density spectra was analyzed. Quality controlled and blended ECMWF winds at six hourly intervals were used in the outer domain to allow the free propagation of swells in the Indian Ocean basin. The Southern Ocean experiences rapid moving meso-scale synoptic storms, where the movements of these storms were analyzed and the resulting swell propagation direction toward

north Indian Ocean was investigated. The WAM4.5.3 model was used to compute the wave parameters in the outer domain and SWAN model in the intermediate domain, with forcing from blended ECMWF winds in both cases. A high resolution unstructured mesh SWAN run forced with WRF winds tuned to simulate land and sea breeze events for coastal Kalpakkam was performed in the inner domain. The model WRF has been configured for the specific site Kalpakkam for operational mesoscale weather forecast. This model has proved its efficacy and robustness in simulating land and sea breeze events successfully in coastal Kalpakkam. During the month of September 2008, the coastal wind system was dominated by land breeze event (about 55%), followed by winds almost parallel to the coast (39% occurrence) and sea breeze conditions were not conducive. The resultant variance energy density spectrum computed from SWAN model with two different sets of numerical experiments were further skill assessed. Based on this study, it could be ascertained that modulation effects from long distant swells are quite significant as seen from the computed energy spectra. The resultant energy levels are noticed almost double when the influx of swell propagation is considered in the region of interest. This points out the fact that identification of potential swell generation areas and their propagation in geographic space and time is very vital in context to wave activity in coastal areas. The results obtained through this numerical study is in close conjunction with the report of a recent study which used buoy as the measurement platform to understand the role of swells in modifying the local wind-generated waves. The limitation in this study is that the reported work was carried out for only 1 month. However, it is believed the effect of swells; their intensity and

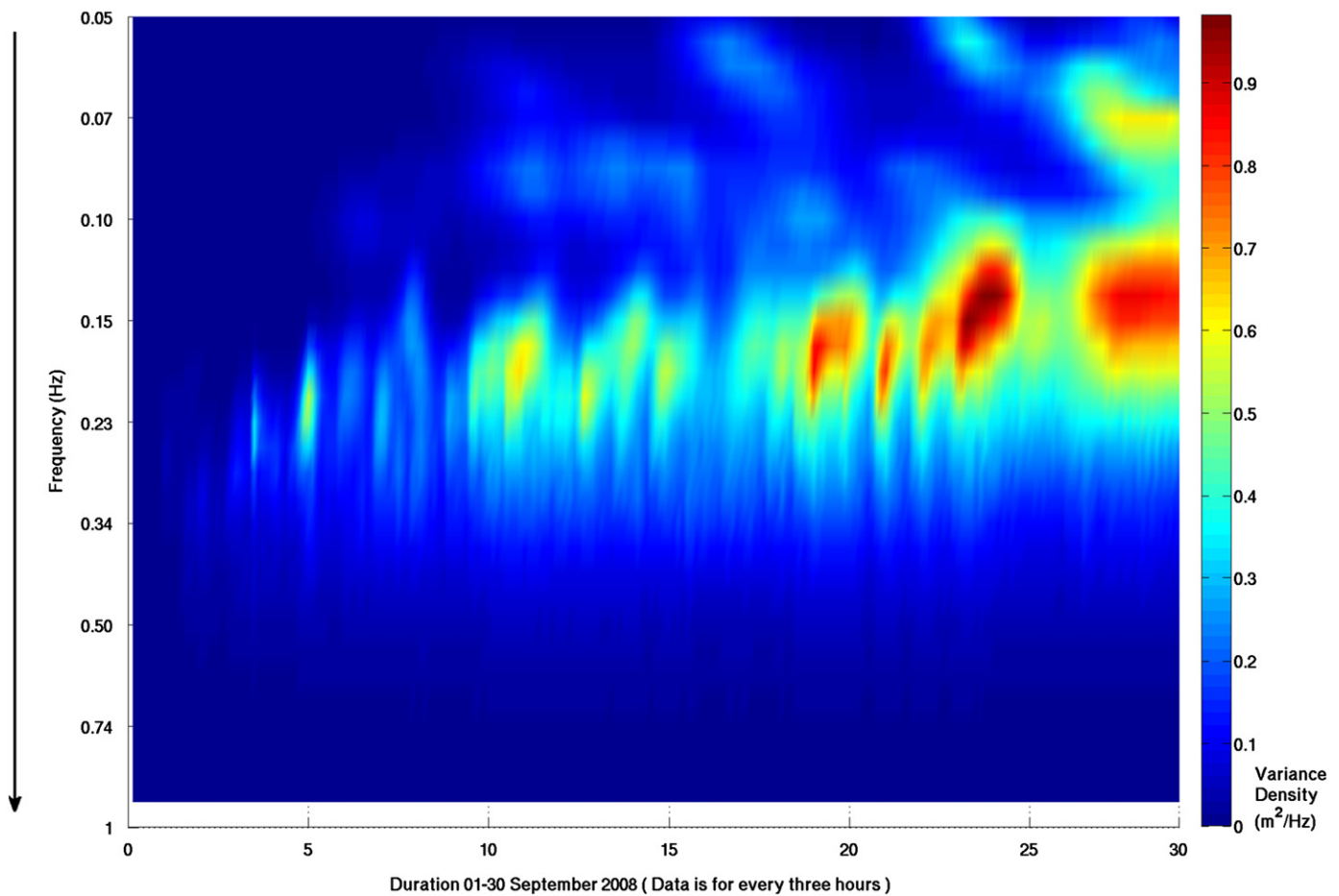


Fig. 12. Evolution of wave variance density spectrum ($\text{m}^2 \text{Hz}^{-1}$) during September 2008 at location-1 considering long swells from Southern Ocean.

movement during various seasons and their validation with directional wave measurements are very important to build a comprehensive database for coastal Kalpakkam.

Acknowledgments

The authors would like to express their sincere gratitude to Indira Gandhi Centre for Atomic Research (IGCAR), Kalpakkam for funding this research project. The computational facilities obtained through this project and constructive research discussions are highly appreciated. The authors like to thank the anonymous reviewers for their constructive suggestions.

References

- Aboobacker, V.M., Rashmi, R., Vethamony, P., Menon, H.B., 2011. On the dominance of pre-existing swells over wind seas along the west coast of India. *Cont. Shelf Res.* 31, 1701–1712.
- Alves, G.M.J.H., 2006. Numerical modeling of ocean swell contributions to the global wind-wave climate. *Ocean Modeling* 11, 98–122.
- Ardhuin, F., O'Reilly, W.C., Herbers, T.H.C., Jessen, P.F., 2003. Swell transformation across the continental shelf. Part I: attenuation and directional broadening. *J. Phys. Oceanogr.* 33 (9), 1921–1939.
- Barber, N.F., Ursell, F., 1948. The generation and propagation of ocean waves and swell. I. Wave periods and velocities. *Philos. Trans. R. Soc. London* 240A, 527–560.
- Bentamy, A., Ayina, H.L., Queffelecoul, P., Croize-Fillon, D., Kerbaol, V., 2007. Improved near real time surface wind resolution over the Mediterranean Sea. *Ocean Sci.* 3, 259–271.
- Bidlot, J., Janssen, P., Abdalla, S., 2005. A revised formulation for ocean wave dissipation in CY29R1. *Mem. Res. Dept. of ECMWF*, April 7, R60.9/JB/0516.
- Booij, N., Ris, R.C., Holthuijsen, L.H., 1999. A third generation wave model for coastal regions, Part I: model description and validation. *J. Geophys. Res.* 104 (C4), 7649–7666.
- Cai, X.M., Steyn, D.G., 2000. Modeling study of sea breezes in a complex coastal environment. *Atmos. Environ.* 34, 2873–2885.
- Chen, G., Belcher, S.E., 2000. Effects of long waves on wind-generated waves. *J. Phys. Oceanogr.* 30 (9), 2246–2256.
- Chen, G., Chapron, B., Ezraty, R., Vandemark, D., 2002. A global view of swell and wind sea climate in the ocean by satellite altimeter and scatterometer. *J. Atmos. Oceanic Technol.* 19 (11), 1849–1859.
- Donelan, M.A., 1987. The effect of swell on the growth of wind waves. *John Hopkins APL Techn. Dig.* 8, 18–23.
- Donelan, M.A., Drennan, W.M., Katsaros, K.B., 1997. The air–sea momentum flux in conditions of wind sea and swell. *J. Phys. Oceanogr.* 27 (10), 2087–2099.
- Grachev, A.A., Fairall, C.W., 2001. Upward momentum transfer in the marine boundary layer. *J. Phys. Oceanogr.* 31, 1698–1711.
- Gross, G., 1986. A numerical study of the land and sea breeze including cloud formation. *Beitr. Phys. Atmos.* 59 (1), 97–114.
- Gunther, J., Hasselmann, S., Janssen, P.A.E.M., 1992. The WAM model Cycle-4, Report No. 4, Hamburg.
- Gunther, H., Behrens, A., 2011. The WAM model—Validation Document Version 4.5.3., Helmholtz-Zentrum Geesthacht, Centre for Materials and Coastal Research, Germany.
- Hanson, J.L., Phillips, O.M., 2001. Automated analysis of ocean surface directional wave spectra. *J. Atmos. Oceanic Technol.*, 277–293.
- Hasselmann, K., Barnett, T.P., Bouws, E., et al., 1973. Measurements of wind-wave growth and swell decay during the Joint North Sea Wave Project (JONSWAP). *Dtsch. Hydrogr. Z. A8* (12), 95.
- Hersbach, H., Janssen, P.A.E.M., 1999. Improvements of the short fetch behavior in the WAM model. *J. Atmos. Oceanic Technol.* 16, 884–892.
- Komen, G.J., Cavaleri, L., Donelan, M., Hasselmann, K., Hasselmann, S., Janssen, P.A.E.M., 1994. *Dynamics and Modeling of Ocean Waves*. Cambridge University Press, pp. 532.
- Lavrenov, I.V., Ocampo-Torres, F.J., 1999. Non-linear energy generation of waves opposite to the wind direction—the wind-driven air–sea interface. In: *Proceedings of the Symposium on the Wind-Driven Air–Sea Interface*, Sydney, Australia, School of Mathematics, The University of New South Wales, pp. 141–150.
- Liu, H.C., Johnny, L., Cheng, A.Y.S., 2001. Internal boundary layer structure under sea breeze conditions in Hong Kong. *Atmos. Environ.* 35, 683–692.
- Mason, D., 1993. On the nonlinear coupling between swell and wind waves. *J. Phys. Oceanogr.* 23, 1249–1258.

- Melas, D., Ziomas, I.C., Zerefos, C.S., 1995. Boundary layer dynamics in an urban coastal environment under sea breeze conditions. *Atmos. Environ.* 29 (24), 3605–3617.
- Munk, W.H., Miller, G.R., Snodgrass, F.E., Barber, N.F., 1963. Directional recording of swell from distant storms. *Philos. Trans. R. Soc. London. Ser. A* 255, 505–584.
- Ogawa, Y., Ohara, T., Wakamatsu, S., et al., 1986. Observation of lake breeze penetration and subsequent development of the thermal internal boundary layer for the NANTICOKE II shoreline diffusion experiment. *Boundary Layer Meteorol.* 35, 207–230.
- Osamu, C., Naito, G., Kobayashi, F., Toritani, H., 1994. Wave trains over the sea due to sea breezes. *Boundary Layer Meteorol.* 70, 329–340.
- Shillington, F.A., 1981. Low frequency 0.045-Hz swell from the Southern Ocean. *Nature* 290, 123–125.
- Sivaramakrishnan, S., Venkatesan, R., 2002. Coastal Atmospheric Boundary Layer Experiment (CABLE-2001). AERB Report, Mumbai, India.
- Skamarock, W.C., Klemp, J.B., Dudhia, J., et al., 2005. A Description of the Advanced Research WRF version 2, NCAR Tech. Note TN-468: 88.
- Smedman, A.S., Larsen, X.G., Hogstrom, U., Kahma, K.K., Pettersson, H., 2003. Effect of sea state on the momentum exchange over the sea during neutral conditions. *J. Geophys. Res.* 108 (C11), 3367.
- Snodgrass, F.E., Groves, G.W., Hasselmann, K.F., Miller, G.R., Munk, W.H., Powers, W.M., 1966. Propagation of swell across the Pacific. *Philos. Trans. R. Soc. London. Ser. A* 259, 431–497.
- Srinivas, C.V., Venkatesan, R., 2005. A simulation study of dispersion of air borne radionuclides from a nuclear power plant under a hypothetical accidental scenario at a tropical coastal site. *Atmos. Environ.* 39 (8), 1497–1511.
- Srinivas, C.V., Venkatesan, R., Somayaji, K.M., Bhagavathsingh, A., 2007. A numerical study of sea breeze circulation observed at a tropical site Kalpakkam on the east coast of India under different synoptic flow situations. *J. Earth Syst. Sci.* 115, 557–574.
- Stopa, J.E., Cheung, K.F., Chen, Y.L., 2011. Assessment of wave energy resources in Hawaii. *Renewable Energy* 36 (2), 554–567.
- Swain, J., 1997. Simulation of wave climate for the Arabian Sea and Bay of Bengal, Ph.D. Thesis., Cochin University of Science and Technology, pp. 142.
- Talke, S.A., Stacey, M.T., 2003. The influence of oceanic swells on flows over an estuarine intertidal mudflat in San Francisco Bay. *Estuarine Coastal Shelf Sci.* 58, 541–554.
- Teixeira, M.A.C., Belcher, S.E., 2002. On the distortion of turbulence by a progressive surface wave. *J. Fluid Mech.* 458, 229–267.
- Thara, V.P., Venkatesan, R., Mursch-Radlgruber, E., Rengarajan, G., Jayanthi, N., 2002. Thermal Internal Boundary Layer characteristics at a tropical coastal site as observed by a mini-SODAR under varying synoptic conditions. *Proc. Indian Acad. Sci.* 111, 63–77.
- Venkatesan, R., Mathiyarasu, R., Somayaji, K.M., 2002. A study of atmospheric dispersion of radionuclides at a coastal site using a modified Gaussian model and a mesoscale sea breeze model. *Atmos. Environ.* 36, 2933–2942.
- Violante-Carvalho, N., Ocampo-Torres, F.J., Robinson, I.S., 2004. Buoy observations of the influence of swell on wind waves in the open ocean. *Appl. Ocean Res.* 26, 49–60.
- Xian, Z., Pielke, R.A., 1991. The effects of width of land-masses on the development of sea breezes. *J. Appl. Meteorol.* 30 (9), 1280–1304.
- Young, I.R., Verhagen, L.A., Banner, M.L., 1995. A note on the bimodal directional spreading of fetch-limited waves. *J. Geophys. Res.* 100, 773–778.